A multi-state Markov chain model for rainfall to be used in optimal operation of rainwater harvesting systems

Abstract

Consideration of rainfall dynamics can rationalize the operation of rainwater harvesting systems. This study aims at establishing a methodology to construct a Markov chain model for time series of rainfall in temperate climates that optimal operation of rainwater harvesting systems is cast in the framework of stochastic dynamic programming. Due to the seasonal climate, the model is time-varying but stationary in each month. The states of the Markov chain are ranges of rainfall depths in 10 minutes. Transition probabilities determining the dynamics of the Markov chain are to be estimated for each month. The occurrence of dry states is frequent enough to estimate the transition probabilities from a dry state empirically. While, on the condition that a wet state is observed, the rainfall depth in the next 10 minutes is assumed to obey to the gamma distribution with two parameters. New formulae, including two exponent parameters, are proposed to relate the conditional mean and variance with the parameters of the gamma distribution. The values of the exponent parameters are identified from sequential searches so that the monthly average rainfall depths in 10 minutes become consistent with the observed ones. Then, a complete set of transition probabilities achieving the mean-reverting property is obtained to establish the Markov chain model. Examples of operating a hypothetical rainwater harvesting system are presented to demonstrate the utility of the Markov chain model in application to optimal management of water resources and stormwater retention in the framework of stochastic dynamic programming. The mean-reverting smooth transition probabilities also contribute to stabilizing the optimal policy.

Keywords: Stochastic time series, Rainfall, Markov chain, Transition probability, Stochastic dynamic programming, Rainwater harvesting

1. Introduction

Rainwater harvesting (RWH) is a technology to collect runoff from a relatively small watershed such as the roof of a building into a reservoir or a storage tank, aiming at the development of renewable water resources to support ecosystem services and human well-being (Barron, 2009). The water harvested during rainfall events can be utilized for satisfying indoor and outdoor demands such as non-potable domestic water supply, gardening in households, and washing of pavements and vehicles (Fernandes et al., 2015). Although water quality control is the major constraint in potable water production (Alim et al., 2020), utilizing RWH systems for urban agriculture is expected to contribute to at least eight of the United Nations' 17 Sustainable Development Goals (Amos et al., 2020). The RWH technology is expected to serve for stormwater retention as well, for instance, reducing site runoff or flood peaks in urban sewage systems (Burns et al., 2015).

Rainfall data is the primary key input for considering the operation of RWH systems. Mitchell (2007) discussed the accuracy of computer-simulated dynamics of RWH systems with different intervals of time series and operational algorithms. The design of optimal tank size for RWH systems should consider the spatial distribution of rainfall patterns (Fonseca et al., 2017). The length and the temporal resolution of rainfall time series to be based on, as well as the operation algorithm, significantly influence the performance assessment of RWH systems (Zhang et al., 2020). However, these studies in the literature lack mathematical rigor in the contexts of stochastic processes and their optimal control, which would determine the rational design and operation of RWH systems.

A Markov chain is a discrete-time stochastic model defined on a space of states, equipped with transition probabilities from a state to another at the next time stage. Application of Markov chains in hydrological engineering includes runoff processes (Lu and Berliner, 1999), standard precipitation index (Paulo et al., 2005), climate change (Cioffi et al., 2017), different weather indices (Lennartsson et al., 2008), agricultural drought (Biamah et al., 2005), and weather generation as in the celebrated WGEN model of Richardson and Wright (1984). Transition probability defining a discrete-time Markov chain involving hydrological phenomena such as precipitation is derived from a model using a probability distribution among Pareto, Lognormal, Weibull, and Gamma distributions (Papalexiou et al., 2013). Applicability of different probability distributions has been examined by many researchers, including the very early study conducted by Markovic (1965). In real-time decision making based on observation, or currently available information, assuming and utilizing Markovian properties are very advantageous in the operation of reservoirs or tanks. Labadie (2004), Rani and Moreira (2010), and Ahmad et al. (2014) reviewed a variety of methods for determining suitable policies for reservoir operation. Among these methods, dynamic programming (DP) is one of the most widely used approaches for seeking the optimal policy for reservoir operation. The rationale of the DP approach is the Bellman's principle of optimality (Bellman, 1957). Yakowitz (1982) reviewed the application of DP techniques to many real-world water resource problems, where the Bellman equations governing the value functions are nonlinear. Developments in computer technology have allowed the DP approach to be applied to increasingly complex stochastic problems (Tejada-Guibert et al., 1993; Tejada-Guibert et al., 1995), referred to as stochastic DP (SDP). Lee and Labadie (2007) demonstrated the applicability of the SDP approach coupled with reinforcement learning for modeling a complex river basin system with two reservoirs. Shokri et al. (2013) determined the optimal policy for the operation of a single reservoir using SDP to meet water demand and to flush sediment simultaneously. Mabaya et al. (2017) derived

reservoir operation rules considering the dual uncertainties of the reservoir storage volume and the pollution due to agrochemicals. Further review of reservoir optimization was also conducted by El-Shafie et al. (2014). More comprehensive hydrological and water requirement dynamics oriented for the operation of RWH systems can be described with continuous-time Markov process models using stochastic differential equations (Unami and Mohawesh, 2018; Unami et al., 2015; Unami et al., 2013). Unami et al. (2013) considered stochastic water demand in a micro-dam irrigation scheme. Unami et al. (2015) proposed to utilize the Langevin equation for representing the general water flow dynamics in RWH systems, and Unami and Mohawesh (2018) showed that the mean-reverting property of the Langevin equation plays an essential role in establishing well-posedness of optimal control problems for operating RWH systems.

This paper proposes a methodology to construct a Markov chain model from time series data of rainfall in order to consider its sequential dynamics, aiming application to optimal operation of a hypothetical RWH system in a study area of Japan. The area is locally known to be anomalously dry but is not well covered by Automated Meteorological Data Acquisition System (AMeDAS), the high-resolution surface observation network developed by Japan Meteorological Agency (2020). The key feature of the methodology, which cannot be found in the literature, is that the Markov chain model with multiple states can be constructed from limited data sources. Therefore, an automated weather station was operated in the study area to obtain time series data, from which the Markov chain model and then the RWH system are developed. Firstly, empirical transition probabilities of rainfall are calculated from the observed time series data. Then, the estimation of transition probabilities is attempted for cases of lacking enough number of data. Although many methods such as the Fourier series fitting by Jimoh and Webster (1999) have been developed for smoothing spurious oscillations of probabilities in hydrology, we consider the use of the gamma distribution that has an advantage of high adaptability with only two parameters. Appropriate values of the parameters are sequentially

searched so that the resulting monthly average rainfall depths become consistent with the observed ones in terms of a metric analogous to the norm in the space of functions of bounded variations. Then, the estimated transition probabilities are incorporated into a discrete-time SDP problem to compute the optimal policy for making the decision on withdrawal of water from the tank in the hypothetical RWH system which is assumed to be installed in the study area. To assure the adequacy of the SDP problem and its numerical solution, stability analysis is implemented as provided in **Appendix B**. Two examples of the hypothetical RWH system are presented. The first one assumes the typical dimensions of an RWH system in a household. The second one consists of a watershed of a plastic pan and a storage tank of a PET bottle to actually implement an in situ experiment.

While, this paper does not address to impacts of climate change on the performance of RWH systems, as in Haque et al. (2016), Zhang et al. (2019), and Adham et al. (2019). The length of the time series data of rainfall is as short as six years, during which the variability of the climate is considered the minimum. Nevertheless, the methodology successfully constructs the Markov chain model from the short time series data. Operation of RWH systems based on SDP as a means of climate change adaptation shall be discussed in future studies, using similar approaches as in Turner et al. (2017), which dealt with hydropower dams, and in Fadhil (2018), which dealt with a multipurpose dam.

2. Materials and methods

2.1. Study area and data acquisition

The study area, which is referred to as the Imago area, has been established in Shiga Prefecture, Japan (Unami and Kawachi, 2005), and its location is shown in the satellite images

(a) and (b) of Figure 1. As can be seen in the satellite image (c) of Figure 1, the Imago area extends over the Nunobiki hill with inland valleys, mostly covered by tea plantations and pastures on the ridges, forests in the slopes, and paddy fields in the valley bottoms (Mabaya et al., 2016). According to the local people's perception, the precipitation in the Imago area is anomalously less in comparison with the neighboring areas. An irrigation project for drought mitigation was implemented during the 1960s, including the development of the canal system to convey water from an adjacent basin to a newly constructed irrigation dam and then to the paddy fields in the Imago area. Buildings such as houses, warehouses, and cattle sheds are scattered, and their number is increasing in these decades. A significant change of the land use after the energy crisis ensuing from the nuclear catastrophe in 2011 is the installation of photovoltaic (PV) power stations converting the forests and the farmlands. Though there is no relevant research on PV power stations affecting stormwater runoff processes, as thoroughly reviewed in Dimond and Webb (2017), it can be easily inferred that such effects are not negligible. These trends in land use imply increases in domestic and livestock water demands as well as the intensification of stormwater runoff, which can be mitigated with the RWH technology applied to the buildings or the PV panels.

The automated weather station equipped with a VAISALA WXT520 weather transmitter was operated from June 4th, 2014 to June 8th, 2020 in a tea plantation at the coordinates 34°57'40.0"N 136°13'18.0"E, recording different weather elements every 10 minutes (photo (d) of Figure 1). The resolution ρ of the rainfall sensor is 0.01 mm. The annual rainfall depths were 1421.04 mm, 1445.08 mm, 1456.36 mm, 1645.82 mm, and 1429.94 mm, corresponding to the years 2015, 2016, 2017, 2018, and 2019, respectively. The maximum of the observed 10-minute rainfall depths during that whole period of six years was 15.54 mm, which was recorded at 17:30 of September 6th, 2014. However, the monthly rainfall is higher in June and July rather than September. A tangible drought period occurred in mid-August of 2016,

and a significant stormwater event destroyed a plot of paddy field on October 6th, 2017. From these episodes, the period is considered to represent rainfall dynamics, including extremes, even though it is too short in the context of statistical hydrology.

While, the nearest AMeDAS station is the Tsuchiyama station, located at the coordinates 34°56'20.1"N 136°16'46.0"E. The distance between the two stations is 5824 m. The annual rainfall depths observed at the Tsuchiyama station were 1631.5 mm, 1449.0 mm, 1613.0 mm, 1832.5 mm, and 1654.0 mm, corresponding to the years 2015, 2016, 2017, 2018, and 2019, respectively. The maximum of the observed 10-minute rainfall depths during that period was 14.0 mm, which was recorded at 10:30 of September 8th, 2016. These values indicate that the rainfall dynamics in the Imago area is quite different from that around the Tsuchiyama station.

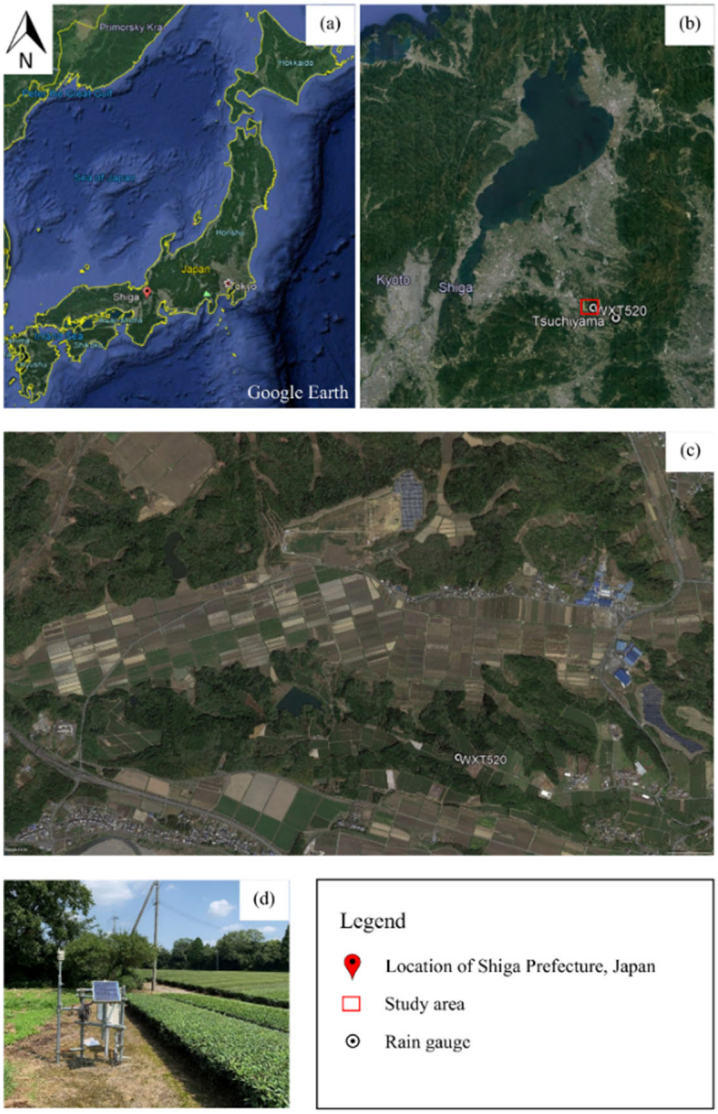

Figure 1: Images describing the Imago area in Shiga Prefecture, Japan: (a) satellite image of Japan, (b) satellite image of Shiga Prefecture, (c) satellite image of the Imago area, (d) photo of the automated weather station in a tea plantation, the images (a-c) were obtained from Google Earth on May 12th, 2020.

2.2. Construction of Markov chain model

In this subsection, we define the multi-state Markov chain model with mathematical rigor. The probability of transition from a state to another is assumed to be year-periodic and constant for each month. The transition probabilities from a wet state are assumed obeying to a gamma distribution, achieving the mean-reverting property of the rainfall depths. The gamma distribution for each wet state and each month is identified so that the resulting monthly average rainfall depths become consistent with the observed ones in terms of a metric analogous to the norm in the space of functions of bounded variations.

The state space Ω of a Markov chain is defined as the set whose elements are the states. An Ω-valued sequence of random variables X_t for $t \in \square$ is called an Ω-valued Markov chain or a Markov chain on Ω, if

$$P\left(X_{t+1} = \omega \middle| X_0 = \omega_0, X_1 = \omega_1, ..., X_t = \omega_t\right) = P\left(X_{t+1} = \omega \middle| X_t = \omega_t\right) \tag{1}$$

for all $t \in \square$ and $\omega_0, \cdots, \omega_t, \omega \in \Omega$, where $P\left(A \middle| B\right)$ represents the conditional probability of the event A given the event B. This equation (1) is usually referred to as the Markov property of the Markov chain X_t.

In our application, the states are the ranges of rainfall depths in the time interval Δt = 10 minutes at the site, which are countable, that is,

$$\Omega = \left\{ \omega_i = \left(i\Delta r - \frac{\Delta r}{2}, i\Delta r + \frac{\Delta r}{2} \right] \right\} \tag{2}$$

for $i \in$ □ with the increment Δr of the states. The Markov chain X_t is equal to ω_i, which is the state representing the i th range of rainfall depths, if the rainfall depth from the time $(t-1)\Delta t$ to the time $t\Delta t$ is in ω_i. The transition probability

$$P_{ij} = P\left(X_{t+1} = \omega_j \middle| X_t = \omega_i\right) \tag{3}$$

where ω_j is the state after the transition, P_{ij} is assumed to be year-periodic and constant for each month *k*.

A process to estimate the transition probabilities is proposed below. Empirical transition probabilities $\tilde{P}_{ij}^{(k)}$ are estimated as

$$\tilde{P}_{ij}^{(k)} = \frac{N_{ij}^{(k)}}{\sum_l N_{il}^{(k)}} \tag{4}$$

where $N_{ij}^{(k)}$ is the number of transitions from the state ω_i to the state ω_j occurred in the month *k*. The denominator $\sum_l N_{il}^{(k)}$ of (4), is equal to the total number of data such that $X_t = \omega_i$ in the month *k*. This empirical estimation is valid for transitions from the state ω_0, which is the dry state, where $\sum_l N_{0l}^{(k)}$ is large enough. While, as there are very few or no observed cases of $X_t = \omega_i$ for $i > 0$, empirical transition probabilities for $i > 0$ exhibit spurious oscillations with respect to the state number j after transition or cannot be calculated. Hence, we examine an alternative method to assume that the rainfall depth *r* from the time $t\Delta t$ to the time $(t+1)\Delta t$, namely in the next Δt, for each ω_i obeys to the gamma distribution whose cumulative density function is

$$P\left(r < x \middle| X_t = \omega_i\right) = \frac{\gamma(\alpha, \beta x)}{\Gamma(\alpha)} = \int_0^x \frac{\beta^\alpha r^{\alpha-1} \exp(-\beta r)}{\Gamma(\alpha)} \mathrm{d}r \tag{5}$$

where x is a generic rainfall depth, α is the shape parameter, β is the scale parameter, Γ is the Gamma function, γ is the lower incomplete gamma function given by

$$\gamma(\alpha,\beta x)=(\beta x)^{\alpha}\,\Gamma(\alpha)\exp(-\beta x)\sum_{n=0}^{\infty}\frac{(\beta x)^{n}}{\Gamma(\alpha+n+1)}. \tag{6}$$

The parameters α and β satisfy

$$\alpha=\frac{\left(\mathrm{E}\left[r\middle|X_t=\omega_i\right]\right)^2}{\mathrm{Var}\left[r\middle|X_t=\omega_i\right]} \tag{7}$$

and

$$\beta=\frac{\mathrm{E}\left[r\middle|X_t=\omega_i\right]}{\mathrm{Var}\left[r\middle|X_t=\omega_i\right]}, \tag{8}$$

respectively. Now, to determine the values of the parameters α and β using (7) and (8), the conditional expectation and variance need to be evaluated from the available observed time series data. For that purpose, we arbitrarily propose the formulae

$$\mathrm{E}\left[r\middle|X_t=\omega_i\right]=\left(\frac{i\Delta r}{\mathrm{E}_{\mathrm{wet}}[r]}\right)^{p_{\mathrm{E}}}\mathrm{E}_{\mathrm{wet}}[r] \tag{9}$$

and

$$\mathrm{Var}\left[r\middle|X_t=\omega_i\right]=\left(\frac{i\Delta r}{\mathrm{E}_{\mathrm{wet}}[r]}\right)^{p_{\mathrm{Var}}}\mathrm{Var}_{\mathrm{wet}}[r] \tag{10}$$

where p_{E} and p_{Var} are exponent parameters, $\mathrm{E}_{\mathrm{wet}}[r]=\mathrm{E}\left[r\middle|X_t\neq\omega_0\right]$ is the expectation of rainfall depths in the next Δt on the condition that a wet state is observed for each month, and $\mathrm{Var}_{\mathrm{wet}}[r]=\mathrm{Var}\left[r\middle|X_t\neq\omega_0\right]$ is the variance of rainfall depths in the next Δt on the condition that a wet state is observed for each month. These formulae (9) and (10) imply that the conditional expectation and variance are monotone, convex functions of the conditioning rainfall depth, which is approximately represented by $i\Delta r$. Each of the exponent parameters

controls the convexity of the monotone function. The formula (9) also hypothesizes that the rainfall depth in the next Δt is reverting to the monthly mean $\mathrm{E}_{\mathrm{wet}}[r]$ if $p_{\mathrm{E}} < 1$, as the left-hand side of (9) becomes larger and smaller than $\mathrm{E}_{\mathrm{wet}}[r]$ when the conditioning rainfall depth is smaller and larger than $\mathrm{E}_{\mathrm{wet}}[r]$, respectively. As an obvious property of transition probabilities, the matrix P_k whose *ij*-entry is $P_{ij}^{(k)}$ for each month *k* has the maximum eigenvalue 1. The corresponding eigenvector represents equilibrium occurrence probabilities of the states, from which the estimated average rainfall depth $\overline{r}_k^{\mathrm{E}}$ in 10 minutes is evaluated for each month *k*, if the representative rainfall depth of each state is specified. Then, the exponent parameters p_{E} and p_{var} are identified from sequential searches to minimize the deviation $\delta\overline{r}_{\mathrm{BV}}$ defined as

$$\delta\overline{r}_{\mathrm{BV}} = \sum_{k=0}^{k<12} \left| \overline{r}_k^{\mathrm{E}} - \overline{r}_k^{\mathrm{O}} \right| + \sum_{k=0}^{k<12} \left| \left(\overline{r}_k^{\mathrm{E}} - \overline{r}_{\mathrm{mod}(k+1,12)}^{\mathrm{E}} \right) - \left(\overline{r}_k^{\mathrm{O}} - \overline{r}_{\mathrm{mod}(k+1,12)}^{\mathrm{O}} \right) \right| \tag{11}$$

where $\overline{r}_k^{\mathrm{O}}$ is the observed average rainfall depth in 10 minutes for each month *k*. This metric of error, inspired by the norm in the space of functions of bounded variations, takes both of absolute errors and total variations in the monthly average rainfall depths into account.

2.3. Application to optimal operation of a hypothetical RWH system

In order to demonstrate the utility of the Markov chain model, the optimal operation of a hypothetical RWH system is considered in the context of SDP, where the Bellman equation is solved temporally backward to obtain an optimal policy maximizing the expected reward in the future. The representative rainfall depth of each state ω_i is specified as $i\Delta r$, which is the same as the approximating conditional rainfall depth in the formulae (9) and (10). Figure 2 is a schematic sketch of such a system with a tank whose watershed is the roof of a house. The

water balance equation governing the storage volume S_t of the tank at the time $t\Delta t$ is written as

$$S_{t+1} = S_t - Q_{\text{out}} + Q_{\text{in}} \tag{12}$$

where Q_{out} is the volume of water withdrawn from the tank at the time $t\Delta t$ and Q_{in} is the volume of water actually harvested as an inflow into the tank from the time $t\Delta t$ to the time $(t+1)\Delta t$. The withdrawal is controlled as

$$Q_{\text{out}} = \begin{cases} 0 & \text{if } u = 0 \\ \min(Q_{\text{w}}, S_t) & \text{if } u = 1 \end{cases} \tag{13}$$

where $u \in \{0,1\}$ is the decision variable, and Q_{w} is a prescribed maximum volume of water which can be withdrawn from the tank at a time. Namely, a valve installed to an outlet of the tank is closed if $u = 0$ and is open if $u = 1$. While, it is assumed that

$$Q_{\text{in}} = \min\left(A_{\text{e}} \max\left(j\Delta r - r_\theta, 0\right), S_{\max} - \left(S_t - Q_{\text{out}}\right)\right) \tag{14}$$

where A_{e} is the effective surface area of the watershed, $X_{t+1} = \omega_j$, r_θ is a threshold of rainfall depth yielding runoff, and $S_{\max}$ is the maximum storage of the tank. Therefore, S_{t+1} in (12) depends on u and j and is represented as $S_{t+1}(u, j)$. The volume Q_{spill} of spilling water which cannot be harvested is

$$Q_{\text{spill}} = Q_{\text{spill}}\left(t, S_t, X_t, u, X_{t+1}\right) = \max\left(A_{\text{e}} \max\left(j\Delta r - r_\theta, 0\right) - Q_{\text{in}}, 0\right) \tag{15}$$

An SDP problem of practical interest is to maximize the conditional expectation of the storage S_T at a specified terminal time $T\Delta t$, as well as to minimize that of the total volume of spilling water from the time 0 to the time $T\Delta t$, by choosing an optimal u from $\{0,1\}$ at each time $t\Delta t$ $(0 \le t < T)$ depending on S_t and on the state ω_i where $X_t = \omega_i$. Such a map from (t, S_t, X_t) to u is referred to as a policy Π. Here, a reward function to include the two conflicting objectives is set as

$$f\left(t,S_t,X_t\right)=-\sum_{\tau=t}^{\tau<T}Q_{\text{spill}}\left(\tau,S_\tau,X_\tau,u,X_{\tau+1}\right)+S_T\,, \tag{16}$$

and the conditional expectation to be maximized, under the policy Π, is denoted by $\mathrm{E}^{\Pi}\left[f\left(t,S_t,X_t\right)\right]$. The first term of (16) represents the total volume of spilling water from the time $t\Delta t$ to the time $T\Delta t$, while the second term does the storage S_T at the terminal time $T\Delta t$ to be maximized in order to meet any water demand which may occur after $T\Delta t$. According to the Bellman's principle of optimality (Gross, 2016), the value function

$$\Phi(t,S_t,i)=\sup_{\Pi}\mathrm{E}^{\Pi}\left[f\left(t,S_t,X_t\right)\right] \tag{17}$$

where $X_t=\omega_i$ solves the Bellman equation

$$\Phi(t,S_t,i)=\max_{u\in\{0,1\}}\left\{\sum_j P_{ij}\left(-Q_{\text{spill}}\left(t,S_t,i,u,j\right)+\Phi\left(t+1,S_{t+1}\left(u,j\right),j\right)\right)\right\} \tag{18}$$

for any time $t\Delta t$, any storage S_t, and any state ω_i. The trivial terminal condition is prescribed as

$$\Phi(T,S_T,i)=S_T \tag{19}$$

for any $\omega_i\in\Omega$, and therefore the computation of (18) is implemented temporally backward as schematized in Figure 3.

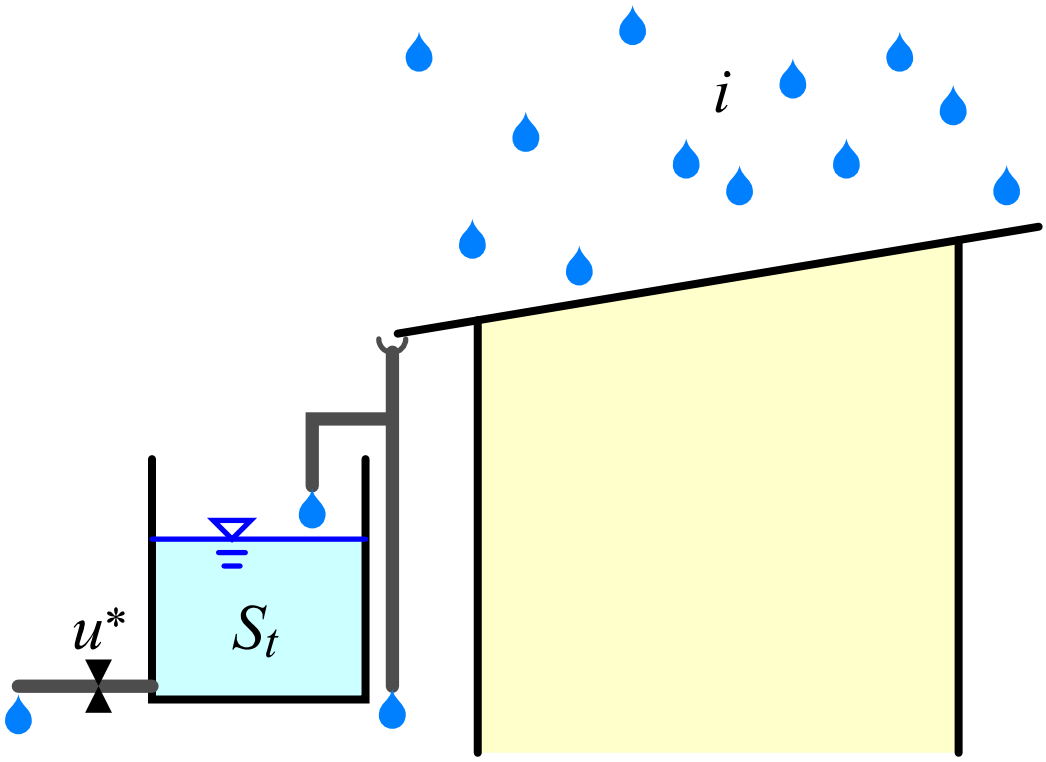

Figure 2: Schematic sketch of the hypothetical RWH system

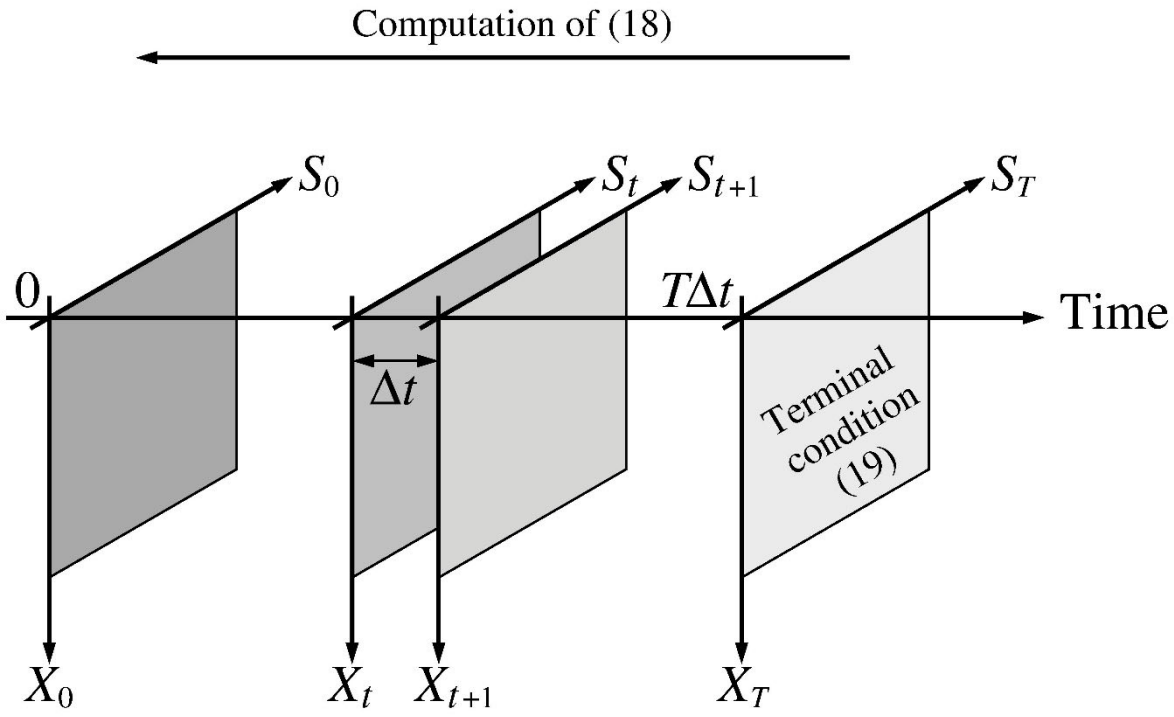

Figure 3: Computational scheme of the Bellman equation

3. Results and discussions

3.1. Estimation of transition probabilities

From the observed time series data of rainfall depths in 10 minutes during the period from June 04, 2014 to June 08, 2020, the number $N_{ij}^{(k)}$ of transitions for each combination of i, j, and k is counted. The increment Δr of the states is set as 0.1 mm, and thus the states of rainfall depths greater than $\Delta r/2 = 0.05$ mm in 10 minutes are regarded as wet. Due to the uneven distribution of data over different i and j, the methods described in subsection *2.2* are adapted to determine $P_{ij}^{(k)}$. For $i = 0$, $\sum_l N_{il}^{(k)}$ is more than 2×10^4 for each month, and $P_{0j}^{(k)} = \tilde{P}_{0j}^{(k)}$ as estimated with (4) is considered acceptable. Transitions between two dry states are significantly large in number for each month. For $i > 0$, the assumption of (5) is made for each month, including the parameters α and β determined by the exponent parameters identified with the formulae (9) and (10). For practical computation, the number of states is limited to $n_r = 400$, and the transition probability $P_{ij_{\max}}^{(k)}$, where $j_{\max}$ is a transited state such that $P_{ij_{\max}}^{(k)} \geq P_{ij}^{(k)}$ for all j, is redefined as

$$P_{ij_{\max}}^{(k)} = 1 - \sum_{j=0}^{j<j_{\max}} P_{ij}^{(k)} - \sum_{j=j_{\max}+1}^{j<n_r} P_{ij}^{(k)} \tag{20}$$

for each i. Sequential searches were initially performed in the region $0.5 \leq p_{\mathrm{E}} < 1.0$ and $-0.50 \leq p_{\mathrm{Var}} \leq 1.50$ with an increment of 0.1 for both parameters. Then, with ad hoc refinements of the region and the increments, the optimal values $p_{\mathrm{E}} = 0.936$ and $p_{\mathrm{Var}} = 0.910$ achieving $\delta\overline{r}_{\mathrm{BV}} = 0.08836$ were obtained. The first and the second terms of the right-hand side of (11) are 0.04209 and 0.04627, respectively, and the resulting value of average annual rainfall

is 1492.20 mm, which is close to the observed 1488.08 mm. The process of sequential searches is depicted in Figure 4. Table 1 summarizes the monthly values of $P_{00}^{(k)}$, which is identical to the empirically estimated $\tilde{P}_{00}^{(k)}$, the key statistics $\mathrm{E}_{\mathrm{wet}}[r]$, $\mathrm{Var}_{\mathrm{wet}}[r]$, and $\overline{r}_k^{\mathrm{O}}$, as well as the optimized $\overline{r}_k^{\mathrm{E}}$. In the summer months from June to September, the continuation of dry states is generally less probable as $P_{00}^{(k)}$ is smaller. The large values of the key statistics imply that intense and irregular rainfall is most significant in August among the summer months. Very good agreement between $\overline{r}_k^{\mathrm{O}}$ and the optimized $\overline{r}_k^{\mathrm{E}}$ can be seen in the months of May, July, and August. As evident from this identification procedure, the validity of the optimized values of the exponent parameters is not universal but limited to this particular case of time series data, Δr, and the number of states for computation.

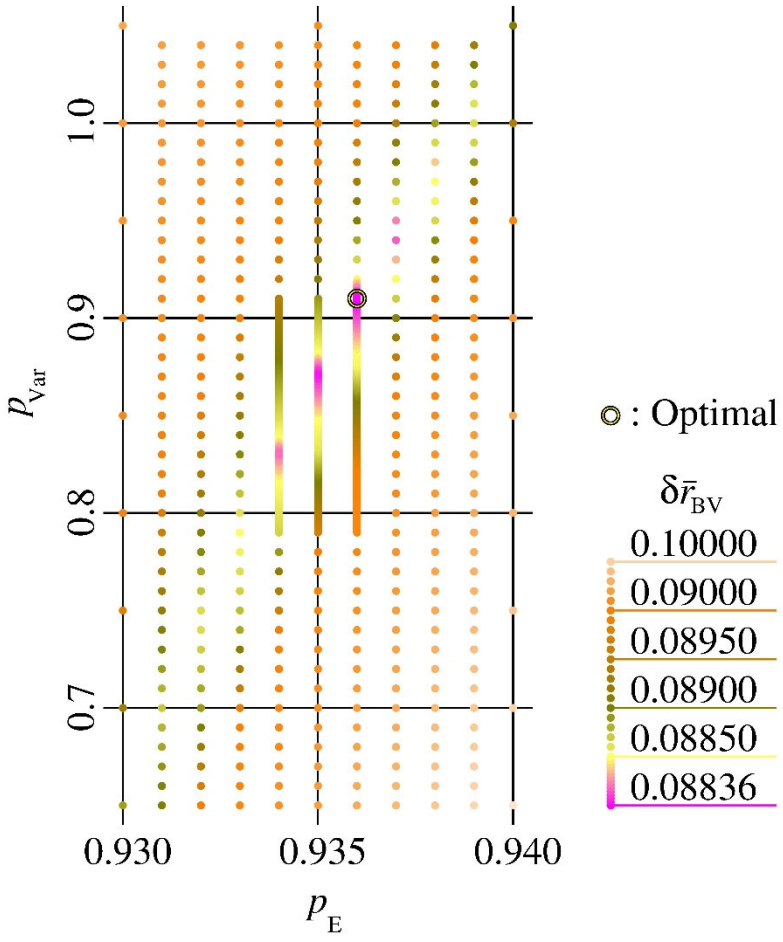

Figure 4: The values of the deviation $\delta\overline{r}_{\mathrm{BV}}$ for different pairs of the exponent parameters

Table 1: $P_{00}^{(k)}$, $\mathrm{E}_{\mathrm{wet}}[r]$, $\mathrm{Var}_{\mathrm{wet}}[r]$, $\overline{r}_k^{\mathrm{O}}$, and the optimized $\overline{r}_k^{\mathrm{E}}$ for each month

	JAN	FEB	MAR	APR	MAY	JUN	JUL	AUG	SEP	OCT	NOV	DEC
$P_{00}^{(k)}$	0.9920	0.9924	0.9900	0.9858	0.9901	0.9855	0.9863	0.9873	0.9856	0.9878	0.9908	0.9910
$\mathrm{E}_{\mathrm{wet}}[r]$	0.2790	0.2976	0.3383	0.3756	0.4577	0.4880	0.5940	0.8217	0.6863	0.5895	0.2780	0.3347
$\mathrm{Var}_{\mathrm{wet}}[r]$	0.1213	0.1360	0.1429	0.2285	0.4614	0.7510	1.0650	1.5237	1.5086	0.6740	0.1246	0.1841
$\overline{r}_k^{\mathrm{O}}$	0.01128	0.01146	0.02141	0.02845	0.02227	0.03748	0.04053	0.04988	0.04674	0.04033	0.01284	0.01503
$\overline{r}_k^{\mathrm{E}}$	0.01423	0.01384	0.02400	0.03308	0.02170	0.03359	0.04053	0.04949	0.04232	0.02953	0.01903	0.01829

3.2. Demonstrative examples of the hypothetical RWH system

SDP is a more rational approach to optimal control problems than simulation, explicitly presenting optimal policies as maps from the state variables to the decision variables. The SDP problem formulated in subsection *2.3* is computationally solved to demonstrate the utility of the Markov chain model. In order to assure the validity of the SDP problem and its numerical solution, stability analysis is implemented for the Bellman equation (18) in terms of the Lipschitz continuity of the Bellman mapping as detailed in **Appendix B**. Such analysis is required for the SDP problem here, because it is discrete-time stochastic and differs from the continuous-time stochastic one (Unami and Mohawesh, 2018) and from discrete-time deterministic one (Unami et al., 2019) in the earlier studies.

The first demonstrative example of the hypothetical RWH system referred to as Case 1, assumes the dimensions of $A_{\mathrm{e}} = 200$ m^2, $S_{\max} = 2$ m^3, $Q_{\mathrm{w}} = 2$ m^3, and $r_\theta = 1$ mm. Setting $T = 144$ time stages makes the terminal time $T\Delta t = 24$ hours. The domain of storage volume is divided into 100 subdomains of an equal volume of 0.02 m^3. Figure 5 shows the optimal policy at the initial time computed over the storage volume-rainfall depth state domain for each

month. Generally, the valve should be closed while the rainfall depth is less, considerably depending on the storage volume; the upper limits of the rainfall depth to close the valve are mostly monotone decreasing functions of the storage volume. The valve should be closed even if there is no rain and the tank is full in the months of January and February, but not in the other months. For more quantitative discussion, the values of the computed value function for $S_0 = 0$ and different states of i = 0, 10, 20, 50, 100, and 399 are shown in Table 2. In contrast to the optimal policy, the value function is the least sensitive to the storage volume at the initial time 0, and therefore the values for $S_0 > 0$ are not presented. The values of $\Phi(0,0,0)$, which is the maximized expectation of the reward function on the condition that the tank is empty and no rain in Δt is observed at $t = 0$, vary differently from any quantity among the months in Table 1, due to the subtle trade-off between spilling and storage of water. For larger conditional rainfall depths, the annual patterns of $\Phi(0,0,i)$ exhibit monomodal variation with the bottom in August, where the rainfall is the most intense and irregular, with the slight anomaly in December as in $\mathrm{E}_{\mathrm{wet}}[r]$ and $\mathrm{Var}_{\mathrm{wet}}[r]$ if $i > 20$. This can be explained by the dominance of the spilling water in the reward function, which is more likely due to the higher possibility of high rainfall depths in the summer months.

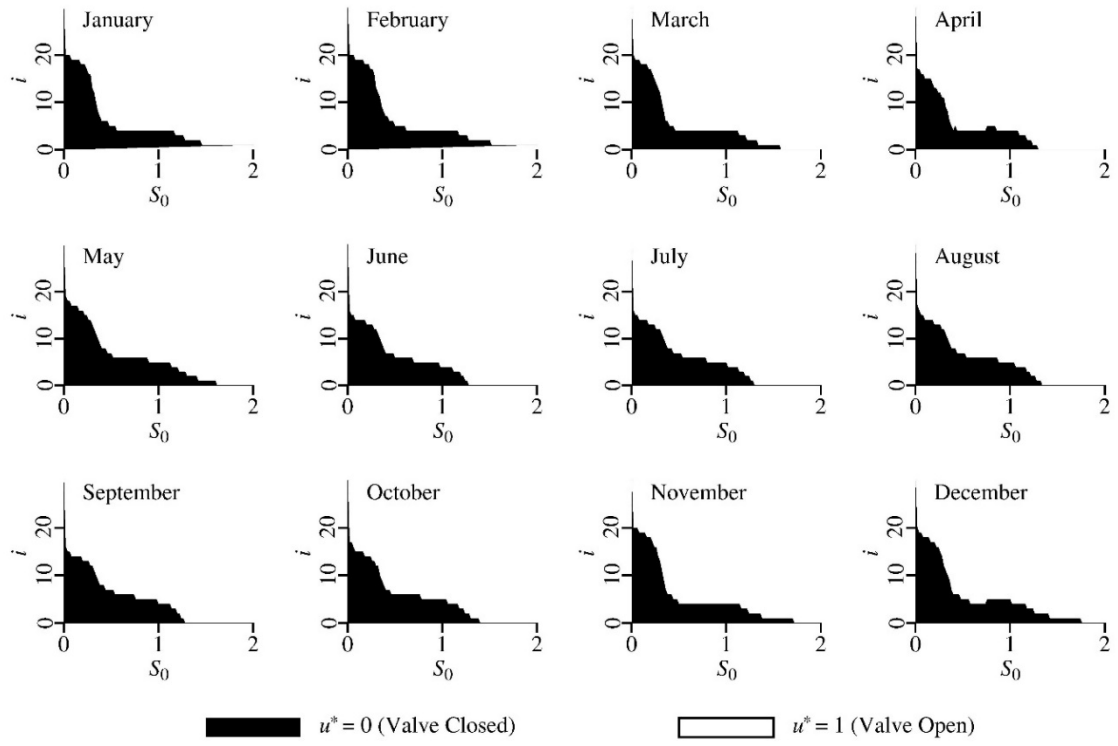

Figure 5: The optimal policy at the initial time 0 computed over the domain of storage volume (m^3) and rainfall depth state for each month: Case 1.

Table 2: Representative values of the computed value function for each month

	JAN	FEB	MAR	APR	MAY	JUN	JUL	AUG	SEP	OCT	NOV	DEC
Φ(0, 0, 10)	0.6878	0.6888	0.6771	0.6830	0.6296	0.4863	0.3539	0.1751	0.2229	0.5391	0.6785	0.6951
Φ(0, 0, 20)	0.6814	0.6801	0.6692	0.6542	0.5308	0.3065	0.1121	-0.1432	-0.0903	0.3880	0.6712	0.6761
Φ(0, 0, 50)	0.6119	0.5976	0.5886	0.4743	0.1073	-0.3525	-0.7229	-1.1959	-1.1164	-0.1972	0.5970	0.5413
Φ(0, 0, 100)	-0.2075	-0.2637	-0.3070	-0.6007	-1.3074	-2.0167	-2.6263	-3.4441	-3.2463	-1.8723	-0.2298	-0.4360
Φ(0, 0, 399)	-12.19	-12.47	-12.95	-13.63	-14.92	-15.44	-16.51	-18.55	-17.15	-16.41	-12.20	-13.05

The second demonstrative example of the hypothetical RWH system referred to as Case 2, consists of a plastic pan and a storage tank of a PET bottle. The pan and the bottle determine the dimensions of $A_e = 0.216$ m^2, $S_{max} = 2$ L, $Q_w = 2$ L, and $r_\theta = 0$ mm. The terminal time is

set as $T\Delta t = 2$ hours with $T = 12$ time stages. The domain of storage volume is divided into 100 subdomains of an equal volume of 20 mL. Figure 6 shows the optimal policy at each time stage for the month of July computed over the storage volume-rainfall depth state domain. Similarly to the first example, the upper limits of the rainfall depth to close the valve appear as mostly monotone decreasing functions of the storage volume at each time stage. The differences in the optimal policy are irregular among the time stages and noticeable at the last two time stages $t = 10$ and $t = 11$. The in situ experiment was implemented beside the automated weather station in the study area on July 3rd, 2020, setting 16:10 (GMT+09:00) as the initial time, with fully manual operation, as can be seen in the video provided as supplementary material. Table 3 shows the performance of the hypothetical RWH system along the trajectory actually realized. As the optimal policy directed to close the valve $\left(u^* = 0\right)$ for all the time stages, no positive Q_{out} occurred. The spillage of water from the tank did not occur as well.

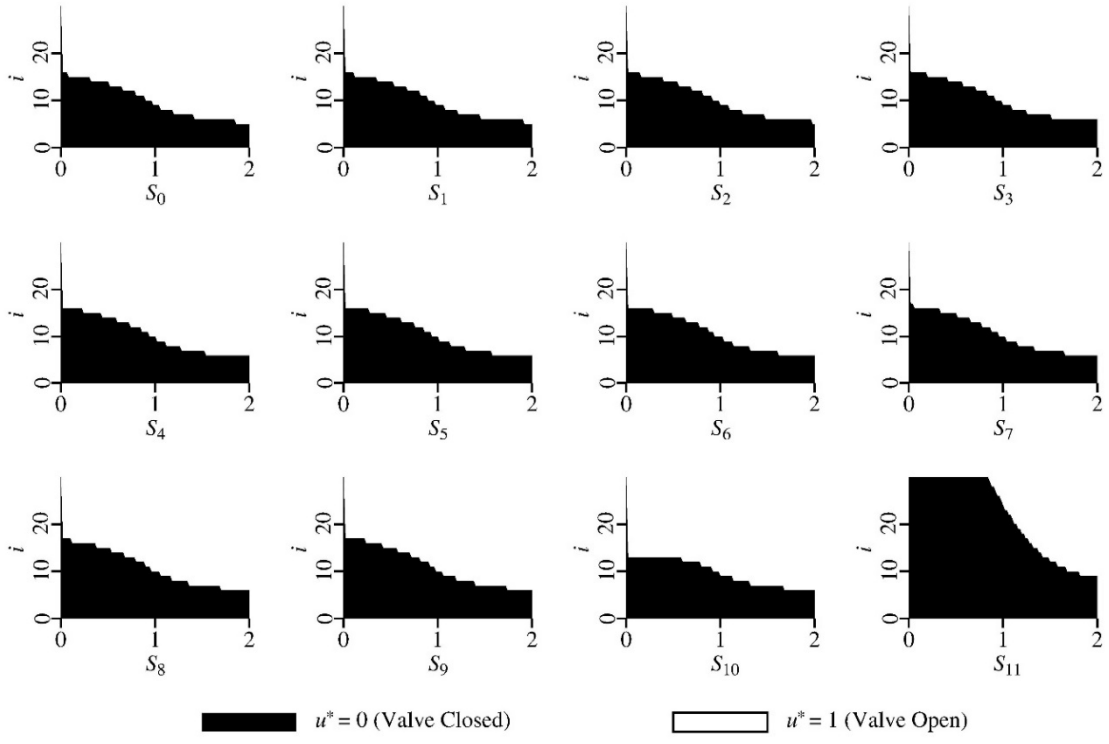

Figure 6: The optimal policy at each time stage for the month of July computed over the domain of storage volume (L) and rainfall depth state: Case 2.

Table 3: Performance of the hypothetical RWH system of Case 2 realized in the in situ experiment

t	S_t (L)	i	$\Phi(t, S_t, i)$ (L)	u^*	Q_{in} (L)
0	0.011	1	0.253	0	0.038
1	0.049	2	0.351	0	0.030
2	0.079	1	0.298	0	0.050
3	0.129	2	0.411	0	0.037
4	0.166	2	0.441	0	0.120
5	0.286	6	0.681	0	0.118
6	0.404	5	0.743	0	0.079
7	0.483	4	0.786	0	0.033
8	0.516	2	0.733	0	0.030
9	0.546	1	0.688	0	0.020
10	0.566	1	0.720	0	0.038
11	0.604	2	0.963	0	0.005
12	0.609	0	0.609	Sum	0.598

4. Conclusions

The Markov chain model for rainfall has been established for the anomalously dry Imago area of Shiga Prefecture, Japan, considering the probability law of transition from one state to another. Empirical transition probabilities from a dry state were computed from the observed time series data, while those from a wet state were estimated with the gamma distribution. The new formulae to determine the parameters in the gamma distribution included the two exponent parameters, taking the mean-reverting property of the rainfall depths into account. The exponent parameters were identified from the sequential searches to minimize the deviation $\delta\overline{r}_{\text{BV}}$ so that the resulting monthly average rainfall depths become consistent with the observed ones. The eigenvector of the matrix of transition probabilities verified the identified values. The examples of operating the hypothetical RWH system are presented to demonstrate the utility of the Markov chain model in application to optimal management of water resources and stormwater retention in

the framework of SDP. In the computed optimal policies, the upper limits of the rainfall depth to close the valve appeared as mostly monotone decreasing functions of the storage volume.

The proposed methodology to construct the Markov chain model from limited data sources is suitable for rainfall dynamics in temperate climates like Japan, where the smooth distribution of the transition probabilities over different i and j does not cause any serious problem. Another drastic methodology might be required to deal with singularity, such as abrupt onsets of dry or wet seasons occurring in arid and semi-arid climates. The treatment of (20) might overestimate the effect of the mean-reverting but would become negligible if n_r was large enough. The adequacy of $i\Delta r$ representing ω_i would also improve with larger n_r and smaller Δr. Another major limitation of this first-order Markov chain model is the incapability of capturing the memory effect of the time series. The authors are currently tackling more sophisticated reservoir operation problems based on Markov chain models of higher-order involving the fractional calculus (Unami et al., 2021).

In practice, the operation of RWH systems, according to scientifically deduced optimal policies, will achieve a better trade-off between water supply and flood control. Therefore, government subsidies for the RWH technology shall put more emphasis on implementing such optimal policies, rather than on installing the RWH facilities as currently subsidized in some local governments in Japan.

Acknowledgment

This research is funded by Grants-in-Aid for Scientific Research No. 16KT0018 and No. 19KK0167 from the Japan Society for the Promotion of Science (JSPS) and by ISHIZUE 2020 of Kyoto University Research Development Program.

Appendix A. Data availability

The data that support the findings of this study are available from the corresponding author upon reasonable request.

Appendix B. Stability analysis for the Bellman equation

In order to assure the validity of the SDP problem and its numerical solution, stability analysis is implemented for the Bellman equation (18) in terms of the Lipschitz continuity of the Bellman mapping here.

For each t such that $0 \le t < T$, the Bellman equation (18) prescribes the Bellman mapping $v^t(S,i)$ as

$$v^t(S,i) = \max_{u\in\{0,1\}} \left\{ \sum_j P_{ij}^{(k)} \left(-Q_{\text{spill}}\left(S,u,j\right) + v^{t+1}\left(\sigma\left(S,u,j\right),j\right)\right)\right\} \tag{21}$$

where

$$Q_{\text{spill}}\left(S,u,j\right) = Q_{\text{spill}}\left(t,S,i,u,j\right) \tag{22}$$

and

$$\sigma\left(S,u,j\right) = S - Q_{\text{out}}\left(S,u\right) + Q_{\text{in}}\left(S,u,j\right). \tag{23}$$

For $t = T$, let

$$v^T(S,i) = S \tag{24}$$

as in the terminal condition (19) of the Bellman equation.

An upper bound of $\left|v^t\left(S,i\right)\right|$, not depending on S, is denoted by $b^t\left(i\right)$ for $0 \le t \le T$. At the terminal time, $b^T\left(i\right) = S_{\max}$. An upper bound of $\left|Q_{\text{spill}}\left(S,u,j\right)\right|$, depending on neither S nor u, is denoted by $b^{\text{Q}}\left(j\right)$. Let L^{Q} be a Lipschitz constant satisfying

$$\sup_i \sum_j P_{ij}^{(k)} \left|Q_{\text{spill}}\left(S_{\text{A}},u,j\right) - Q_{\text{spill}}\left(S_{\text{B}},u,j\right)\right| \le L^{\text{Q}} \left|S_{\text{A}} - S_{\text{B}}\right| \tag{25}$$

and L^{S} be another Lipschitz constant satisfying

$$\left|\sigma\left(S_{\text{A}},u,j\right) - \sigma\left(S_{\text{B}},u,j\right)\right| \le L^{\text{S}} \left|S_{\text{A}} - S_{\text{B}}\right| \tag{26}$$

for any pair of S_{A} and S_{B} in $\left[0, S_{\max}\right]$.

Theorem 1. $b^{\text{Q}}\left(j\right) = A_{\text{e}} j\Delta r$, $L^{\text{Q}} = 1$, *and* $L^{S} = 1$.

Proof. Let $q = A_{\text{e}} \max\left(j\Delta r - r_\theta, 0\right)$. Without loss of generality, we assume $S_{\text{B}} \le S_{\text{A}}$ for $S_{\text{A}}, S_{\text{B}} \in \left[0, S_{\max}\right]$.

If $u = 0$, then $Q_{\text{out}} = 0$, $Q_{\text{in}}\left(S\right) = \min\left(q, S_{\max} - S\right)$, and $Q_{\text{spill}}\left(S,u,j\right) = \max\left(q,0\right) = q$. Thus, $\left|Q_{\text{spill}}\left(S,u,j\right)\right| \le q$ and $\left|Q_{\text{spill}}\left(S_{\text{A}},u,j\right) - Q_{\text{spill}}\left(S_{\text{B}},u,j\right)\right| = 0$. Note that $\sigma\left(S\right) = S + Q_{\text{in}}(S)$ and $\sigma\left(S_{\text{A}}\right) - \sigma\left(S_{\text{B}}\right) = S_{\text{A}} - S_{\text{B}} + Q_{\text{in}}(S_{\text{A}}) - Q_{\text{in}}(S_{\text{B}})$. There are three cases regarding $Q_{\text{in}}\left(S\right)$:

- Case q-0-1: $q \le S_{\max} - S_{\text{A}} \le S_{\max} - S_{\text{B}}$
- Case q-0-2: $S_{\max} - S_{\text{A}} \le q \le S_{\max} - S_{\text{B}}$
- Case q-0-3: $S_{\max} - S_{\text{A}} \le S_{\max} - S_{\text{B}} \le q$

Consequently, $Q_{\text{in}}\left(S_{\text{A}}\right)$, $Q_{\text{in}}\left(S_{\text{B}}\right)$, and $\sigma\left(S_{\text{A}}\right) - \sigma\left(S_{\text{B}}\right)$ are calculated as in the table below:

	Case q-0-1	Case q-0-2	Case q-0-3
$Q_{\text{in}}\left(S_{\text{A}}\right)$	q	$S_{\max} - S_{\text{A}}$	$S_{\max} - S_{\text{A}}$
$Q_{\text{in}}\left(S_{\text{B}}\right)$	q	q	$S_{\max} - S_{\text{B}}$
$\sigma\left(S_{\text{A}}\right) - \sigma\left(S_{\text{B}}\right)$	$S_{\text{A}} - S_{\text{B}}$	$S_{\max} - S_{\text{B}} - q$ [1)]	0

1) Case q-0-2: $0 \le S_{\max} - S_B - q$;
Case q-0-2: $-q \le -S_{\max} + S_A$, $S_{\max} - S_B - q \le S_A - S_B$

Since $0 \le \sigma(S_A) - \sigma(S_B) \le S_A - S_B$ for all of the three cases, $|\sigma(S_A) - \sigma(S_B)| \le |S_A - S_B|$.

If $u = 1$, then $Q_{out} = Q_{out}(S) = \min(Q_w, S)$. There are three cases regarding $Q_{in}(S)$:

- Case Q_w-a: $Q_w \le S_B \le S_A$
- Case Q_w-b: $S_B \le Q_w \le S_A$
- Case Q_w-c: $S_B \le S_A \le Q_w$

Consequently, $Q_{out}(S_A)$, $Q_{out}(S_B)$, $S_{\max} - (S_A - Q_{out}(S_A))$, and $S_{\max} - (S_B - Q_{out}(S_B))$ are calculated as in the table below:

	$Q_{out}(S_A)$	$Q_{out}(S_B)$	$S_{\max} - (S_A - Q_{out}(S_A))$	$S_{\max} - (S_B - Q_{out}(S_B))$
Case Q_w-a	Q_w	Q_w	$S_{\max} - S_A + Q_w \le S_{\max}$	$S_{\max} - S_B + Q_w \le S_{\max}$
Case Q_w-b	Q_w	S_B	$S_{\max} - S_A + Q_w \le S_{\max}$	$S_{\max}$
Case Q_w-c	S_A	S_B	$S_{\max}$	$S_{\max}$

Furthermore, there are four cases regarding $Q_{in}(S)$:

- Case q-1-1: $q \le S_{\max} - S_A + Q_w \le S_{\max} - S_B + Q_w \le S_{\max}$
- Case q-1-2: $S_{\max} - S_A + Q_w \le q \le S_{\max} - S_B + Q_w \le S_{\max}$
- Case q-1-3: $S_{\max} - S_A + Q_w \le S_{\max} - S_B + Q_w \le q \le S_{\max}$
- Case q-1-4: $S_{\max} - S_A + Q_w \le S_{\max} - S_B + Q_w \le S_{\max} \le q$

Consequently, eight variables are calculated as in the tables below:

$Q_{in}(S_A) = \min(q, S_{\max} - (S_A - Q_{out}(S_A)))$

	Case q-1-1	Case q-1-2	Case q-1-3	Case q-1-4
Case Q_w-a	q	$S_{\max} - S_A + Q_w$	$S_{\max} - S_A + Q_w$	$S_{\max} - S_A + Q_w$
Case Q_w-b	q	$S_{\max} - S_A + Q_w$	$S_{\max} - S_A + Q_w$	$S_{\max} - S_A + Q_w$

Case Q_{w}-c	q	q	q	$S_{\max}$

$Q_{\mathrm{in}}\left(S_{\mathrm{B}}\right)=\min\left(q, S_{\max}-\left(S_{\mathrm{B}}-Q_{\mathrm{out}}\left(S_{\mathrm{B}}\right)\right)\right)$

	Case q-1-1	Case q-1-2	Case q-1-3	Case q-1-4
Case Q_{w}-a	q	q	$S_{\max}-S_{\mathrm{B}}+Q_{\mathrm{w}}$	$S_{\max}-S_{\mathrm{B}}+Q_{\mathrm{w}}$
Case Q_{w}-b	q	q	$S_{\max}-S_{\mathrm{B}}+Q_{\mathrm{w}}$	$S_{\max}$
Case Q_{w}-c	q	q	q	$S_{\max}$

$Q_{\mathrm{spill}}\left(S_{\mathrm{A}}, u, j\right)=\max\left(q-Q_{\mathrm{in}}\left(S_{\mathrm{A}}\right), 0\right)$

	Case q-1-1	Case q-1-2	Case q-1-3	Case q-1-4
Case Q_{w}-a	0	$q-S_{\max}+S_{\mathrm{A}}-Q_{\mathrm{w}}$ 2)	$q-S_{\max}+S_{\mathrm{A}}-Q_{\mathrm{w}}$ 2)	$q-S_{\max}+S_{\mathrm{A}}-Q_{\mathrm{w}}$ 2)
Case Q_{w}-b	0	$q-S_{\max}+S_{\mathrm{A}}-Q_{\mathrm{w}}$ 2)	$q-S_{\max}+S_{\mathrm{A}}-Q_{\mathrm{w}}$ 2)	$q-S_{\max}+S_{\mathrm{A}}-Q_{\mathrm{w}}$ 2)
Case Q_{w}-c	0	0	0	$q-S_{\max}$

$Q_{\mathrm{spill}}\left(S_{\mathrm{B}}, u, j\right)=\max\left(q-Q_{\mathrm{in}}\left(S_{\mathrm{B}}\right), 0\right)$

	Case q-1-1	Case q-1-2	Case q-1-3	Case q-1-4
Case Q_{w}-a	0	0	$q-S_{\max}+S_{\mathrm{B}}-Q_{\mathrm{w}}$ 3)	$q-S_{\max}+S_{\mathrm{B}}-Q_{\mathrm{w}}$ 3)
Case Q_{w}-b	0	0	$q-S_{\max}+S_{\mathrm{B}}-Q_{\mathrm{w}}$ 3)	$q-S_{\max}$
Case Q_{w}-c	0	0	0	$q-S_{\max}$

$Q_{\mathrm{spill}}\left(S_{\mathrm{A}}, u, j\right)-Q_{\mathrm{spill}}\left(S_{\mathrm{B}}, u, j\right)$

	Case q-1-1	Case q-1-2	Case q-1-3	Case q-1-4
Case Q_{w}-a	0	$q-S_{\max}+S_{\mathrm{A}}-Q_{\mathrm{w}}$ 2,4)	$S_{\mathrm{A}}-S_{\mathrm{B}}$	$S_{\mathrm{A}}-S_{\mathrm{B}}$
Case Q_{w}-b	0	$q-S_{\max}+S_{\mathrm{A}}-Q_{\mathrm{w}}$ 2,4)	$S_{\mathrm{A}}-S_{\mathrm{B}}$	$S_{\mathrm{A}}-Q_{\mathrm{w}}$ 5)
Case Q_{w}-c	0	0	0	0

$\sigma\left(S_{\mathrm{A}}\right)=S_{\mathrm{A}}-Q_{\mathrm{out}}\left(S_{\mathrm{A}}\right)+Q_{\mathrm{in}}\left(S_{\mathrm{A}}\right)$

	Case q-1-1	Case q-1-2	Case q-1-3	Case q-1-4
Case Q_{w}-a	$S_{\mathrm{A}}-Q_{\mathrm{w}}+q$	$S_{\max}$	$S_{\max}$	$S_{\max}$
Case Q_{w}-b	$S_{\mathrm{A}}-Q_{\mathrm{w}}+q$	$S_{\max}$	$S_{\max}$	$S_{\max}$
Case Q_{w}-c	q	q	q	$S_{\max}$

$\sigma\left(S_{\mathrm{B}}\right)=S_{\mathrm{B}}-Q_{\mathrm{out}}\left(S_{\mathrm{B}}\right)+Q_{\mathrm{in}}\left(S_{\mathrm{B}}\right)$

	Case q-1-1	Case q-1-2	Case q-1-3	Case q-1-4
Case Q_{w}-a	$S_{\mathrm{B}}-Q_{\mathrm{w}}+q$	$S_{\mathrm{B}}-Q_{\mathrm{w}}+q$	$S_{\max}$	$S_{\max}$
Case Q_{w}-b	q	q	$S_{\max}$	$S_{\max}$
Case Q_{w}-c	q	q	q	$S_{\max}$

$\sigma\left(S_{\mathrm{A}}\right)-\sigma\left(S_{\mathrm{B}}\right)$

	Case q-1-1	Case q-1-2	Case q-1-3	Case q-1-4
Case Q_{w}-a	$S_{\mathrm{A}}-S_{\mathrm{B}}$	$S_{\max}-S_{\mathrm{B}}+Q_{\mathrm{w}}-q$ [6]	0	0
Case Q_{w}-b	$S_{\mathrm{A}}-Q_{\mathrm{w}}$ [7]	$S_{\max}-q$ [8]	0	0
Case Q_{w}-c	0	0	0	0

[2] Case q-1-2/3/4: $0 \le q-S_{\max}+S_{\mathrm{A}}-Q_{\mathrm{w}}$;
Case Q_{w}-a/b: $0 \le S_{\max}-S_{\mathrm{A}}+Q_{\mathrm{w}}$, $q-S_{\max}+S_{\mathrm{A}}-Q_{\mathrm{w}} \le q$

[3] Case q-1-3/4: $0 \le q-S_{\max}+S_{\mathrm{B}}-Q_{\mathrm{w}}$;
Case Q_{w}-a/b: $0 \le S_{\max}-S_{\mathrm{B}}+Q_{\mathrm{w}}$, $q-S_{\max}+S_{\mathrm{B}}-Q_{\mathrm{w}} \le q$

[4] Case q-1-2: $q-S_{\max}+S_{\mathrm{A}}-Q_{\mathrm{w}} \le S_{\mathrm{A}}-S_{\mathrm{B}}$

[5] Case Q_{w}-b: . $-Q_{\mathrm{w}} \le -S_{\mathrm{B}}$., $S_{\mathrm{A}}-Q_{\mathrm{w}} \le S_{\mathrm{A}}-S_{\mathrm{B}}$

[6] Case q-1-2: $0 \le S_{\max}-S_{\mathrm{B}}+Q_{\mathrm{w}}-q$;
Case q-1-2: $-q \le -S_{\max}+S_{\mathrm{A}}-Q_{\mathrm{w}}$, $S_{\max}-S_{\mathrm{B}}+Q_{\mathrm{w}}-q \le S_{\mathrm{A}}-S_{\mathrm{B}}$

[7] Case Q_{w}-b: $Q_{\mathrm{w}} \le S_{\mathrm{A}}$, $0 \le S_{\mathrm{A}}-Q_{\mathrm{w}}$;
Case Q_{w}-b: $-Q_{\mathrm{w}} \le -S_{\mathrm{B}}$, $S_{\mathrm{A}}-Q_{\mathrm{w}} \le S_{\mathrm{A}}-S_{\mathrm{B}}$

[8] Case q-1-2: $q \le S_{\max}$, $0 \le S_{\max}-q$;
Case q-1-2: $-q \le -S_{\max}+S_{\mathrm{A}}-Q_{\mathrm{w}}$, $S_{\max}-q \le S_{\mathrm{A}}-Q_{\mathrm{w}} \le S_{\mathrm{A}}-S_{\mathrm{B}}$

Since $0 \le Q_{\mathrm{spill}}\left(S,u,j\right) \le q$, $0 \le Q_{\mathrm{spill}}\left(S_{\mathrm{A}},u,j\right)-Q_{\mathrm{spill}}\left(S_{\mathrm{B}},u,j\right) \le S_{\mathrm{A}}-S_{\mathrm{B}}$, and $0 \le \sigma\left(S_{\mathrm{A}}\right)-\sigma\left(S_{\mathrm{B}}\right) \le S_{\mathrm{A}}-S_{\mathrm{B}}$ for all of the twelve cases, $\left|Q_{\mathrm{spill}}\left(S,u,j\right)\right| \le q$, $\left|Q_{\mathrm{spill}}\left(S_{\mathrm{A}},u,j\right)-Q_{\mathrm{spill}}\left(S_{\mathrm{B}},u,j\right)\right| \le \left|S_{\mathrm{A}}-S_{\mathrm{B}}\right|$, and $\left|\sigma\left(S_{\mathrm{A}}\right)-\sigma\left(S_{\mathrm{B}}\right)\right| \le \left|S_{\mathrm{A}}-S_{\mathrm{B}}\right|$.

Finally, we conclude that $b^{\mathrm{Q}}\left(j\right)=A_{\mathrm{e}}j\Delta r$, $L^{\mathrm{Q}}=1$, and $L^{\mathrm{S}}=1$. □

The stability of the Bellman equation is stated as the Lipschitz continuity of the Bellman mapping shown in the Theorem 2 below.

Theorem 2. *The Bellman mapping* $v^0(S,i)$ *at* $t=0$ *is Lipschitz continuous with respect to* S *and* i. *Namely, there exist real Lipschitz constants* L *and* B *such that*

$$\left|v^0(S_{\mathrm{A}},i_{\mathrm{A}})-v^0(S_{\mathrm{B}},i_{\mathrm{B}})\right|\le L\left|S_{\mathrm{A}}-S_{\mathrm{B}}\right|+B\left|i_{\mathrm{A}}-i_{\mathrm{B}}\right| \tag{27}$$

for any pair of S_{A} *and* S_{B} *in* $\left[0,S_{\max}\right]$ *and for any pair of* i_{A} *and* i_{B} *in* □ .

Proof. Assume $v^t(S_{\mathrm{A}},i)\ge v^t(S_{\mathrm{B}},i)$ and let u^* be the optimal decision variable when $S_t=S_{\mathrm{A}}$ such that $v^t(S_{\mathrm{A}},i)=\sum_j P_{ij}^{(k)}\left(-Q_{\mathrm{spill}}\left(S_{\mathrm{A}},u^*,j\right)+v^{t+1}\left(\sigma\left(S_{\mathrm{A}},u^*,j\right),j\right)\right)$. If there exists a real number L^s such that $\left|v^s(S_{\mathrm{A}},i)-v^s(S_{\mathrm{B}},i)\right|\le L^s\left|S_{\mathrm{A}}-S_{\mathrm{B}}\right|$ for $t<\forall s\le T$, then

$$\begin{aligned}
\left|v^t(S_{\mathrm{A}},i)-v^t(S_{\mathrm{B}},i)\right| &\le v^t(S_{\mathrm{A}},i)-v^t(S_{\mathrm{B}},i)\\
&\le v^t(S_{\mathrm{A}},i)-\sum_j P_{ij}^{(k)}\left(-Q_{\mathrm{spill}}\left(S_{\mathrm{B}},u^*,j\right)+v^{t+1}\left(\sigma\left(S_{\mathrm{B}},u^*,j\right),j\right)\right)\\
&=\sum_j P_{ij}^{(k)}\left(-Q_{\mathrm{spill}}\left(S_{\mathrm{A}},u^*,j\right)+Q_{\mathrm{spill}}\left(S_{\mathrm{B}},u^*,j\right)\right)\\
&\quad+\sum_j P_{ij}^{(k)}\left(v^{t+1}\left(\sigma\left(S_{\mathrm{A}},u^*,j\right),j\right)-v^{t+1}\left(\sigma\left(S_{\mathrm{B}},u^*,j\right),j\right)\right)\\
&\le\sum_j P_{ij}^{(k)}\left|Q_{\mathrm{spill}}\left(S_{\mathrm{A}},u^*,j\right)-Q_{\mathrm{spill}}\left(S_{\mathrm{B}},u^*,j\right)\right| \qquad (28)\\
&\quad+\sum_j P_{ij}^{(k)}\left|v^{t+1}\left(\sigma\left(S_{\mathrm{A}},u^*,j\right),j\right)-v^{t+1}\left(\sigma\left(S_{\mathrm{B}},u^*,j\right),j\right)\right|\\
&\le L^{\mathrm{Q}}\left|S_{\mathrm{A}}-S_{\mathrm{B}}\right|+\sum_j P_{ij}^{(k)}L^{t+1}\left|\sigma\left(S_{\mathrm{A}},u^*,j\right)-\sigma\left(S_{\mathrm{B}},u^*,j\right)\right|\\
&\le L^{\mathrm{Q}}\left|S_{\mathrm{A}}-S_{\mathrm{B}}\right|+L^{\mathrm{S}}L^{t+1}\left|S_{\mathrm{A}}-S_{\mathrm{B}}\right|\\
&=\left(L^{\mathrm{Q}}+L^{\mathrm{S}}L^{t+1}\right)\left|S_{\mathrm{A}}-S_{\mathrm{B}}\right|
\end{aligned}$$

implying that

$$L^t=L^{\mathrm{Q}}+L^{\mathrm{S}}L^{t+1}=L^{\mathrm{Q}}\sum_{\tau=t}^{\tau<T}L^{\mathrm{S}^{\tau-t}}+L^{\mathrm{S}^{T-t}}L^T \tag{29}$$

where $L^t=T-t+1$ because $L^{\mathrm{Q}}=1$ and $L^{\mathrm{S}}=1$ as in Theorem 1, and because of $L^T=1$. Assume that $b^s(i)$ is finite for $t<\forall s\le T$. Then,

$$\begin{aligned}\left|v^t(S,i)\right| &= \left|\sum_j P_{ij}^{(k)}\left(-Q_{\text{spill}}\left(S,u^*,j\right)+v^{t+1}\left(\sigma\left(S,u^*,j\right),j\right)\right)\right| \\ &\le \sum_j P_{ij}^{(k)}\left(\left|Q_{\text{spill}}\left(S,u^*,j\right)\right|+\left|v^{t+1}\left(\sigma\left(S,u^*,j\right),j\right)\right|\right) \\ &\le \sum_j P_{ij}^{(k)}\left(b^{\text{Q}}\left(j\right)+b^{t+1}\left(j\right)\right)\end{aligned} \tag{30}$$

from where it turns out that

$$\mathbf{b}^t = \mathrm{P}_k\mathbf{b}^{\text{Q}} + \mathrm{P}_k\mathbf{b}^{t+1} = \left(\sum_{\tau=t}^{\tau<T}\mathrm{P}_k^{\ \tau-t+1}\right)\mathbf{b}^{\text{Q}} + \mathrm{P}_k^{\ T-t}\mathbf{b}^T \tag{31}$$

where $\mathbf{b}^{\text{Q}} = \begin{pmatrix}\vdots\\ b^{\text{Q}}(i)\\ \vdots\end{pmatrix}$, and $\mathbf{b}^t = \begin{pmatrix}\vdots\\ b^t(i)\\ \vdots\end{pmatrix}$. Let $B^{\text{Q}} = \sup_i \sum_j P_{ij}^{(k)} b^{\text{Q}}\left(j\right)$ and $B^t = \sup_i \sum_j P_{ij}^{(k)} b^t\left(j\right)$.

With $b^{\text{Q}}\left(j\right) = A_{\text{e}} j\Delta r$ as in Theorem 1, it can be seen that B^{Q} and thus B^t are finite if and only if $p_{\text{E}} < 1$ and that B^t linearly increases with respect to $\left(T-t\right)$. Assume $v^t(S,i_{\text{A}}) \ge v^t(S,i_{\text{B}})$ and let u^* be the optimal decision variable when $i = i_{\text{A}}$ such that $v^t(S,i_{\text{A}}) = \sum_j P_{i_{\text{A}}j}^{(k)}\left(-Q_{\text{spill}}\left(S,u^*,j\right)+v^{t+1}\left(\sigma\left(S,u^*,j\right),j\right)\right)$. Then,

$$\begin{aligned}\left|v^t(S,i_{\text{A}})-v^t(S,i_{\text{B}})\right| &\le v^t(S,i_{\text{A}})-v^t(S,i_{\text{B}}) \\ &\le v^t(S,i_{\text{A}})-\sum_j P_{i_{\text{B}}j}^{(k)}\left(-Q_{\text{spill}}\left(S,u^*,j\right)+v^{t+1}\left(\sigma\left(S,u^*,j\right),j\right)\right) \\ &= \sum_j\left(P_{i_{\text{A}}j}^{(k)}-P_{i_{\text{B}}j}^{(k)}\right)\left(-Q_{\text{spill}}\left(S,u^*,j\right)+v^{t+1}\left(\sigma\left(S,u^*,j\right),j\right)\right) \\ &\le \sum_j\left|P_{i_{\text{A}}j}^{(k)}-P_{i_{\text{B}}j}^{(k)}\right|\left(\left|Q_{\text{spill}}\left(S,u^*,j\right)\right|+\left|v^{t+1}\left(\sigma\left(S,u^*,j\right),j\right)\right|\right) \\ &\le \sum_j\left|P_{i_{\text{A}}j}^{(k)}-P_{i_{\text{B}}j}^{(k)}\right|\left(b^{\text{Q}}\left(j\right)+b^{t+1}\left(j\right)\right)\end{aligned} \tag{32}$$

Furthermore,

$$\begin{aligned}&\sum_j\left|P_{i_{\text{A}}j}^{(k)}-P_{i_{\text{B}}j}^{(k)}\right|\left(b^{\text{Q}}\left(j\right)+b^{t+1}\left(j\right)\right) \\ &\le \sum_j\left|P_{i_{\text{A}}j}^{(k)}\right|\left(b^{\text{Q}}\left(j\right)+b^{t+1}\left(j\right)\right)+\sum_j\left|P_{i_{\text{B}}j}^{(k)}\right|\left(b^{\text{Q}}\left(j\right)+b^{t+1}\left(j\right)\right) = 2\left(B^{\text{Q}}+B^{t+1}\right)\end{aligned} \tag{33}$$

but if $i_{\text{A}} = i_{\text{B}}$ then

$$\sum_j \left| P_{i_A j}^{(k)} - P_{i_B j}^{(k)} \right| \left(b^{\mathrm{Q}}(j) + b^{t+1}(j) \right) = 0 . \tag{34}$$

Therefore,

$$\left| v^t(S, i_A) - v^t(S, i_B) \right| \le 2\left(B^{\mathrm{Q}} + B^{t+1} \right) \left| i_A - i_B \right| . \tag{35}$$

Finally, the left-hand side of the asserted inequality (27) is evaluated as

$$\begin{aligned} \left| v^0(S_A, i_A) - v^0(S_B, i_B) \right| &= \left| v^0(S_A, i_A) - v^0(S_B, i_A) + v^0(S_B, i_A) - v^0(S_B, i_B) \right| \\ &\le \left| v^0(S_A, i_A) - v^0(S_B, i_A) \right| + \left| v^0(S_B, i_A) - v^0(S_B, i_B) \right| , \\ &\le (T+1) \left| S_A - S_B \right| + 2\left(B^{\mathrm{Q}} + B^{t+1} \right) \left| i_A - i_B \right| \end{aligned} \tag{36}$$

and the inequality holds with $L = T + 1$ and $B = 2\left(B^{\mathrm{Q}} + B^{t+1} \right)$. The both Lipschitz constants L and B linearly increase with respect to T, and they are finite whenever T is finite. □

References

Adham, A., Wesseling, J.G., Abed, R., Riksen, M., Ouessar, M., Ritsema, C.J., 2019. Assessing the impact of climate change on rainwater harvesting in the Oum Zessar watershed in Southeastern Tunisia. Agric. Water Manage., 221: 131-140. DOI:10.1016/j.agwat.2019.05.006

Ahmad, A., El-Shafie, A., Razali, S.F.M., Mohamad, Z.S., 2014. Reservoir optimization in water resources: a review. Water Resour. Manage., 28(11): 3391-3405. DOI:10.1007/s11269-014-0700-5

Alim, M.A., Rahman, A., Tao, Z., Samali, B., Khan, M.M., Shirin, S., 2020. Suitability of roof harvested rainwater for potential potable water production: A scoping review. J. Clean. Prod., 248. DOI:10.1016/j.jclepro.2019.119226

Amos, C.C., Rahman, A., Gathenya, J.M., Friedler, E., Karim, F., Renzaho, A., 2020. Roof-harvested rainwater use in household agriculture: contributions to the sustainable development goals. Water, 12(2). DOI:10.3390/w12020332

Barron, J., 2009. Rainwater harvesting: a lifeline for human well-being. DEP/1162/NA, Stockholm Environment Institute, Nairobi, Kenya.

Bellman, R., 1957. Dynamic programming. Princeton University Press, Princeton.

Biamah, E.K., Sterk, G., Sharma, T.C., 2005. Analysis of agricultural drought in Iiuni, Eastern Kenya: application of a Markov model. Hydrol. Processes, 19(6): 1307-1322. DOI:10.1002/hyp.5556

Burns, M.J., Fletcher, T.D., Duncan, H.P., Hatt, B.E., Ladson, A.R., Walsh, C.J., 2015. The performance of rainwater tanks for stormwater retention and water supply at the household scale: an empirical study. Hydrol. Processes, 29(1): 152-160. DOI:10.1002/hyp.10142

Cioffi, F., Conticello, F., Lall, U., Marotta, L., Telesca, V., 2017. Large scale climate and rainfall seasonality in a Mediterranean Area: Insights from a non-homogeneous Markov model applied to the Agro-Pontino plain. Hydrol. Processes, 31(3): 668-686. DOI:10.1002/hyp.11061

Dimond, K., Webb, A., 2017. Sustainable roof selection: Environmental and contextual factors to be considered in choosing a vegetated roof or rooftop solar photovoltaic system. Sustain. Cities Soc., 35: 241-249. DOI:10.1016/j.scs.2017.08.015

El-Shafie, A., El-Shafie, A.H., Mukhlisin, M., 2014. New approach: integrated risk-stochastic dynamic model for dam and reservoir optimization. Water Resour. Manage., 28(8): 2093-2107. DOI:10.1007/s11269-014-0596-0

Fadhil, R.M., 2018. Daily operation of Bukit Merah Reservoir with stochastic dynamic programming under the impact of climate change, Universiti Putra Malaysia, 220 pp.

Fernandes, L.F.S., Terencio, D.P.S., Pacheco, F.A.L., 2015. Rainwater harvesting systems for low demanding applications. Sci. Total Environ., 529: 91-100. DOI:10.1016/j.scitotenv.2015.05.061

Fonseca, C.R., Hidalgo, V., Diaz-Delgado, C., Vilchis-Frances, A.Y., Gallego, I., 2017. Design of optimal tank size for rainwater harvesting systems through use of a web application and geo-referenced rainfall patterns. J. Clean. Prod., 145: 323-335. DOI:10.1016/j.jclepro.2017.01.057

Gross, E., 2016. On the Bellman's principle of optimality. Physica A, 462: 217-221. DOI:10.1016/j.physa.2016.06.083

Haque, M.M., Rahman, A., Samali, B., 2016. Evaluation of climate change impacts on rainwater harvesting. J. Clean. Prod., 137: 60-69. DOI:10.1016/j.jclepro.2016.07.038

Japan Meteorological Agency, 2020. Meteorological observation data. Japan Meteorological Agency.

Jimoh, O.D., Webster, P., 1999. Stochastic modelling of daily rainfall in Nigeria: intra-annual variation of model parameters. J. Hydrol., 222(1-4): 1-17. DOI:10.1016/S0022-1694(99)00088-8

Labadie, J.W., 2004. Optimal operation of multireservoir systems: State-of-the-art review. J. Water Resour. Plan. Manage., 130(2): 93-111. DOI:10.1061/(ASCE)0733-9496(2004)130:2(93)

Lee, J.H., Labadie, J.W., 2007. Stochastic optimization of multireservoir systems via reinforcement learning. Water Resour. Res., 43(11). DOI:10.1029/2006wr005627

Lennartsson, J., Baxevani, A., Chen, D.L., 2008. Modelling precipitation in Sweden using multiple step markov chains and a composite model. J. Hydrol., 363(1-4): 42-59. DOI:10.1016/j.jhydrol.2008.10.003

Lu, Z.Q., Berliner, L.M., 1999. Markov switching time series models with application to a daily runoff series. Water Resour. Res., 35(2): 523-534. DOI:10.1029/98WR02686

Mabaya, G., Unami, K., Fujihara, M., 2017. Stochastic optimal control of agrochemical pollutant loads in reservoirs for irrigation. J. Clean. Prod., 146: 37-46. DOI:10.1016/j.jclepro.2016.05.108

Mabaya, G., Unami, K., Yoshioka, H., Takeuchi, J., Fujihara, M., 2016. Robust optimal diversion of agricultural drainage water from tea plantations to paddy fields during rice growing seasons and non-rice growing seasons. Paddy Water Environ., 14(1): 247-258. DOI:10.1007/s10333-015-0494-y

Markovic, R.D., 1965. Probability functions of best fit to distributions of annual precipitation and runoff, Colorado State University, Colorado.

Mitchell, V.G., 2007. How important is the selection of computational analysis method to the accuracy of rainwater tank behaviour modelling? Hydrol. Processes, 21(21): 2850-2861. DOI:10.1002/hyp.6499

Papalexiou, S.M., Koutsoyiannis, D., Makropoulos, C., 2013. How extreme is extreme? An assessment of daily rainfall distribution tails. Hydrol. Earth Syst. Sci., 17(2): 851-862. DOI:10.5194/hess-17-851-2013

Paulo, A.A., Ferreira, E., Coelho, C., Pereira, L.S., 2005. Drought class transition analysis through Markov and Loglinear models, an approach to early warning. Agric. Water Manage., 77(1-3): 59-81. DOI:10.1016/j.agwat.2004.09.039

Rani, D., Moreira, M.M., 2010. Simulation–optimization modeling: a survey and potential application in reservoir systems operation. Water Resour. Manage., 24(6): 1107-1138. DOI:10.1007/s11269-009-9488-0

Richardson, C.W., Wright, D.A., 1984. WGEN: A model for generating daily weather variables. US Department of Agriculture, Agricultural Research Service Washington, DC, USA.

Shokri, A., Bozorg-Haddad, O., Mariño, M.A., 2013. Reservoir operation for simultaneously meeting water demand and sediment flushing: stochastic dynamic programming approach with two uncertainties. J. Water Resour. Plan. Manage., 139(3): 277-289. DOI:10.1061/(ASCE)WR.1943-5452.0000244

Tejada-Guibert, J.A., Johnson, S.A., Stedinger, J.R., 1993. Comparison of two approaches for implementing multireservoir operating policies derived using stochastic dynamic programming. Water Resour. Res., 29(12): 3969-3980. DOI:10.1029/93WR02277

Tejada-Guibert, J.A., Johnson, S.A., Stedinger, J.R., 1995. The value of hydrologic information in stochastic dynamic programming models of a multireservoir system. Water Resour. Res., 31(10): 2571-2579. DOI:10.1029/95WR02172

Turner, S.W.D., Ng, J.Y., Galelli, S., 2017. Examining global electricity supply vulnerability to climate change using a high-fidelity hydropower dam model. Sci. Total Environ., 590: 663-675. DOI:10.1016/j.scitotenv.2017.03.022

Unami, K., Fadhil, R.M., Kamal, M.R., 2021. Rainfall-runoff models with fractional derivatives applied to Kurau River Basin, Perak, Malaysia. Basrah J. Agric. Sci.: (accepted).

Unami, K., Kawachi, T., 2005. Systematic assessment of flood mitigation in a tank irrigated paddy fields area. Paddy Water Environ, 3(4): 191-199. DOI:10.1007/s10333-005-0022-6

Unami, K., Mohawesh, O., 2018. A unique value function for an optimal control problem of irrigation water intake from a reservoir harvesting flash floods. Stoch. Environ. Res. Risk Assess., 32(11): 3169-3182. DOI:10.1007/s00477-018-1527-z

Unami, K., Mohawesh, O., Fadhil, R.M., 2019. Time periodic optimal policy for operation of a water storage tank using the dynamic programming approach. Appl. Math. Comput., 353: 418-431. DOI:10.1016/j.amc.2019.02.005

Unami, K., Mohawesh, O., Sharifi, E., Takeuchi, J., Fujihara, M., 2015. Stochastic modelling and control of rainwater harvesting systems for irrigation during dry spells. J. Clean. Prod., 88: 185-195. DOI:10.1016/j.jclepro.2014.03.100

Unami, K., Yangyuoru, M., Alam, A.H.M.B., Kranjac-Berisavljevic, G., 2013. Stochastic control of a micro-dam irrigation scheme for dry season farming. Stoch. Environ. Res. Risk Assess., 27(1): 77-89. DOI:10.1007/s00477-012-0555-3

Yakowitz, S., 1982. Dynamic programming applications in water resources. Water Resour. Res., 18(4): 673-696. DOI:10.1029/WR018i004p00673

Zhang, S.H., Jing, X.E., Yue, T.J., Wang, J., 2020. Performance assessment of rainwater harvesting systems: Influence of operating algorithm, length and temporal scale of rainfall time series. J. Clean. Prod., 253. DOI:10.1016/j.jclepro.2020.120044

Zhang, S.H., Zhang, J.J., Yue, T.J., Jing, X.E., 2019. Impacts of climate change on urban rainwater harvesting systems. Sci. Total Environ., 665: 262-274. DOI:10.1016/j.scitotenv.2019.02.135